



Experimental evaluation of the effect of air velocity in hybrid solar distiller

Khaoula Hidouri^{a,*}, Ali Benhmidene^a, Mamdouh El Haj Assad^b, Bechir Chouachi^a

^aEngineers National School of Gabès, Analysis Processes Unit, Gabès University, Omar Ibn El Khattab Street, 6029 Gabès, Tunisia, email: khaoula2013@yahoo.fr (K. Hidouri), ali.benhmidene@gmail.com (A. Benhmidene), bechir.chouachi@enig.rnu.tn (B. Chouachi)

^bUniversity of Sharjah Sustainable and Renewable Energy Engineering Department, 27272 Sharjah, UAE, email: massad@sharjah.ac.ae

Received 4 September 2017; Accepted 26 February 2018

ABSTRACT

This paper represents the study of experimental evaluation of hybrid single slope solar still integrated with the heat pump. Which has been carried out at RECAP research unit in ENIGGabès (Latitude 33° 52'53" N and Longitude 10° 05'53" E). The hot air is indented into water within the hybrid solar still with a speed of 0.04–0.08 m/s. The basin area, which has the constant depth. When the air passes through the water, it influences the performance parameters such as the temperatures and different modes of heat transfer rate. The value of convective heat transfer between water and air reaches 2.2 W/m² °C (the theoretical results give good argument with the experimental result as it has only 4% error), between air and glass the convective heat coefficient equal 0.6 W/m² °C (the theoretical values are in the same order as the experiment with a 17% error). The temperature difference between water and inner glass surface, with an addition of dry air inside the basin, will enhance cumulative productivity (P_{cu}) of the hybrid single slope solar still and recorded 16 l/m²-d.

Keywords: Convective heat transfer coefficient; Evaporative heat transfer coefficient; Air velocity; Hybrid distiller integrated with hot air compressor

1. Introduction

The demand for fresh potable water is increasing day by day due to growth in population and industrialization worldwide. Sadly more than one-third of humanity, generally belonging to third world countries, has not enough drinking water. Solutions are systems that lead to better exploitation of human surface water or groundwater, as well as the use of desalination of seawater and emphasis must be given on technological development for making water as reusable using renewable clean energy sources. Desalination of brackish waters or seawater by solar distillation is an operation widely used in arid regions, in small scale due to its low production rate. Many researchers have been reported ways to increase the productivity of solar stills [1–2]. The air flow is one of the most important parameters governing the operation of solar distillers as passive or active. The

installation of the solar distillers with forced convection was carried out by Tiwari and Gupta [3] the purpose of introducing the air into the evaporator to bring the steam into the external heat exchanger, were an efficiency of the system in order of 62% or 5.6 l/m²-d. Simultaneous use of ambient air bubbly and an air pump coupling and that of the ambient with glass cube cooling is intended to increase the productivity by 33.5% up to 47.5% reported by Pandey [4]. Srithar and Rajaseenivasan [5] have carried out an experimental study on water in a solar still, which has been heated directly by solar energy. The air enters the humidifier through the nozzles, mixes with the water, moistens and some of the air were condensed in the glass lid and the remaining air also gets condensed in the dehumidifier. The experimental result gives effect of the solar air heater with and without turbulator. The maximum specific humidity gain has been recorded 0.187 kg_{water}/kg_{air}, while the integrated humidifier with

*Corresponding author.

the solar air heater without turbulator gives maximum specific moisture gain $0.11 \text{ kg}_{\text{water}}/\text{kg}_{\text{air}}$ and peak distillate yield $20.61 \text{ kg}/\text{m}^2$ for a day. Koyuncu [6] have compared several flat plate designs containing one ribbed plate and several glazing configurations and maximum efficient reported at 45.8% for the flat black metal plate with a single polymer glazing, and air passing over the absorber. Matrawy [7] used fins below the absorber plate to enhance heat transfer to the air as it flowed under the absorber but only achieved 50% collector efficiency. Nguyen [8] study experimentally and theoretically two models of a solar distiller with natural convection and another forced with the addition of an air pump. Very complex resolution models have been used. New equations have been used to determine the convective and evaporative transfer coefficients. This study shows a good correlation between that of theoretical and experimental results. Zerrouki et al. [9] have given a numerical study of a capillary film that is in series with a solar still. Phenomena of heat and mass transfer were studied and theoretical results validated with the experimental outcome. With the objective of experimental evaluation Rajasekar et al. [10] have been evaluated a humidification-dehumidification system (HDH). They establish and validate correlation of increasing the relative humidity in the humidifier results enhancement in evaporation efficiency which resultants can improve the distillate output. Kabeel et al. [11] have developed a new summer configuration which can be added to increase the heat transfer between the glass and the basin of distiller unit and it can boost the efficiency of the unit up to 30.6%. Mink et al. [12] have been experimentally evaluated the performance of air blown still with heat recycling. Kabeel et al. [13] have made solar distillers unit, which was capable to has an injection of the hot air bubbles within basin saline water due to which productivity of freshwater reached about $9.36 \text{ l}/\text{m}^2\cdot\text{d}$. Distillate output was recorded 108% higher as compare to the conventional solar distiller unit. Correlation for Lewis number for the evaluation of mass flow rate [14] and effect of different glass orientation on productivity has been discussed [15]. Hybrid solar still integrated with the earth energy was reported by Sodha et al. [16]. Experimental evaluation of integrated solar still using ANN model Theoretical have been reported by Hidouri et al. [17].

Shukla et al. [18] have been realized a system with solar air heating coupling with variable flow rate dependent on solar radiation and air flow. The temperature difference between the ambient and the output are of the order of 35°C . The various experiments showed that $0.09 \text{ kg}/\text{s}$ is an optimum mass flow rate for the conditions tested, thus this value has given maximum energy and exergy efficiency. A experimental study for utilization of hot waste water using long still has been reported by Mishra et al. [19]. A comprehensive review for enhancing the distillate yield using fin, energy storage materials and multi-basin solar still have been discussed by Panchal and Mohan [20].

This paper represents theoretical evaluation and experimental simulation results of newly developed hybrid solar still integrated with the heat pump.

2. Experimental setup

A schematic representation of heat and mass transfer in force circulation mode is shown in Fig.1a, Fig. 1b shows an actual photograph of the experimental test rig. The hybrid distiller unit has made from a stainless steel material of a 3 mm thick sheet, with 0.4 m^2 basin surface area. Table 3 gives the design parameters of the hybrid solar still. An air pump is used for indentation of air within the distiller unit in the basin area. An incident solar radiation has recorded with the help of SP-Light Silicon Pyrano meter. K-type thermocouple sensors and digital temperature indicator and data logger were used for recording different temperatures while the experimentation. Collected condensate yield of hybrid solar still was measured with the help of graduated cylinder.

3. Theoretical background

Energy balance equations for evaluation of the heat and mass transfer coefficients within the hybrid solar still can be written as:

Glass cover equation

$$\frac{dT_g}{dt} = \frac{S_g}{(m_g C_{pg})} (\alpha_g (1 - \phi_g) G + (q_{ew} + q_{r,w-g} + q_{c,w-g}) - q_{r,g-a} - q_{c,g-a}) \quad (1)$$

Evaporator equation

$$\frac{dT_f}{dt} = \frac{S_f}{(m_e C_{pe})} (q_{cw-f} + q_{ew,w-f} - q_{ev,f}) \quad (2)$$

Water equation

$$\frac{dT_w}{dt} = \frac{S_w}{(m_w C_{pw})} ((1 - \alpha_g)(1 - \phi_g)\alpha_w G + q_{c,b-w} + q_c - q_{r,w-g} - q_{ew} - q_{c,w-g} - q_{r,w-f} - q_{ew,w-f} - q_{c,w-f}) \quad (3)$$

Basin equation

$$\frac{dT_b}{dt} = \frac{S_b}{(m_b C_{pb})} ((1 - \alpha_g)(1 - \phi_g)(1 - \alpha_w)\alpha_b G - q_{c,b-w} - q_{losses}) \quad (4)$$

Yield equation

$$\frac{dm_e}{dt} = \frac{q_{ew}}{L_v} \quad (5)$$

Matlab software was used for evaluation of different mode of heat and mass transfer (conduction, convection, radiation, and evaporation), variation in temperature within the distiller unit and the distillate flow rate.

In the forced convection dominates, the relation between Nusselt (Nu), Reynolds (Re) and Prandtl (Pr) was given by J. A. Duffie [21].

$$Nu = \frac{h_{cwf} L}{k_i} = 0.683 Re^{0.466} Pr^{1/3} \quad (6)$$

Rate convective heat transfer between water basin and flow rate of air can be written as:

$$q_{cwf} = 3.908 \left(\frac{V}{L} \right)^{1/2} (T_w - T_g) \quad (7)$$

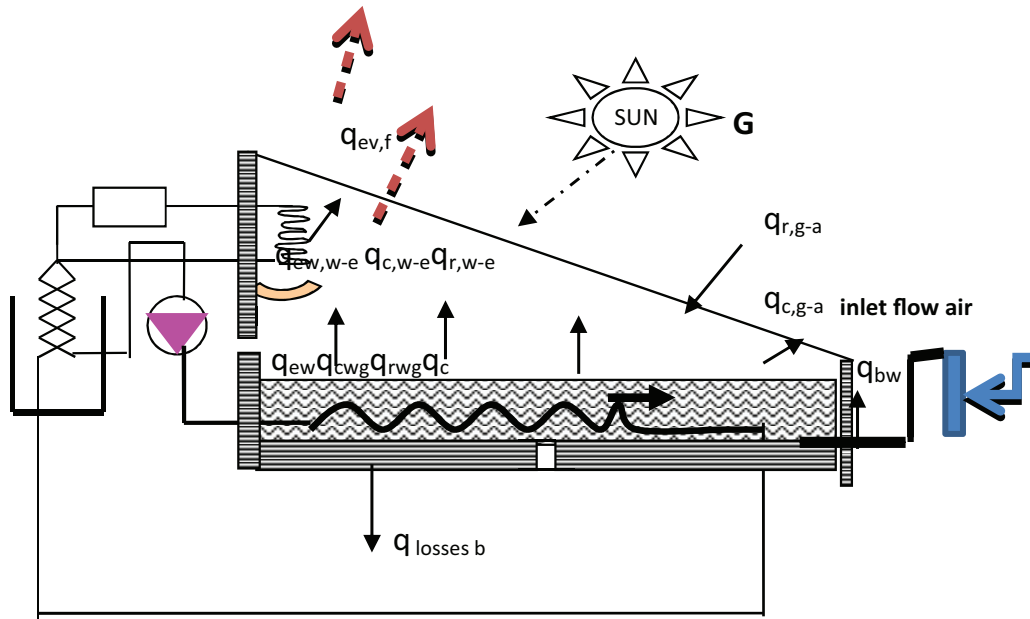


Fig. 1a. Schematic representation of heat and mass transfer process within the developed single slope hybrid solar still.



Fig. 1b. Actual photograph of hybrid single slope solar still coupled with an air pump.

Rate convective heat transfer between the flow rate of air and the cover can be written as:

$$q_{cfs} = 2.785 \left(\frac{V^{0.8}}{L^{0.2}} \right) (T_f - T_g) \quad (8)$$

The water will condense on the inner cover surface when the temperature of air flow is higher than cover temperature; distilled water (m_{ewg}) can be calculated from:

$$m_{ewg} = \frac{q_{con-g}}{h_{fg}} \quad (9)$$

where h_{fg} is the heat vaporization.

The condensate heat transfer rate between the flow and cover:

$$q_{con-g} = h_{con-g} (T_f - T_g) \quad (10)$$

where,

$$Nu = \frac{h_{con-g} L}{k_i} = 0.943 \left(\frac{g^2 \sin \beta h_{fg} L^3}{\mu k_i \Delta T} \right)^{1/4} \quad (11)$$

using the properties of the air at $T_f = 40^\circ\text{C}$;

$$q_{con-g} = 70.93 \left(\frac{\sin \beta}{\Delta T L} \right)^{1/4} \quad (12)$$

4. Uncertainty analysis

The measurements of the parametric variables, air flow rate, water temperature, water level and relative air humidity and temperature within the basin inlet and on the water surface, were taken during the experiments. The water temperature in the basin was measured using the thermometer-Pt100, which works in the range from -20 to $+260^\circ\text{C}$ with an uncertainty of 2.6%. The relative humidity and temperature of air streams were measured using 2 thermo-hygrometers which work in the range from 0 to 100% RH and from -40 to $+120^\circ\text{C}$ and its uncertainty is 1.4% tabulated in Table 1, Table 2 shows operating characteristics of different components.

5. Experimental results and discussion

During the month of July 2015 working hour incident solar radiation on glass cover surface was recorded with the help of Pyrano meter and shown in Fig. 2 along with the theoretical evaluation with the Matlab with respect to time. The maximum solar intensity of incident radiation were recorded at an interval of 12 h and 14 h around $900\text{W}/\text{m}^2$. It shows good agreement between the measured and calculated values for a sunny day.

Table1
Details of measuring equipment and its range along with their accuracy

| Measuring equipment's | Number | Range | Accuracy |
|---|--------|-------------|----------------|
| K-type thermocouple | 5 | -200–1250°C | -0.2–+2°C |
| Digital differential pressure manometer | 2 | (+)-2 bar | -2–+2% |
| Digital thermo-hygrometer | 2 | 0–100% RH | -1.4 – +1.4%RH |
| Thermometer-Pt100 | 4 | -20–+260C | 2.6% |

Table 2
Operating characteristics of glass, basin and water

| Parameter | Value |
|--|--------|
| Specific mass of glass m_g , kg/m ² | 10.12 |
| Specific mass of water m_w , kg/m ² | 20.6 |
| Density of water d , kg/dm ³ | 1 |
| Specific mass of basin m_b , kg/m ² | 15.6 |
| Calorific heat capacity of glass C_{pg} , J/kg°C | 800 |
| Calorific heat capacity of water C_{pw} , J/kg°C | 4178 |
| Calorific heat capacity of basin C_{pb} , J/kg°C | 480 |
| Absorbability of glass cover α_g | 0.075 |
| Water absorbability α_w | 0.05 |
| Basin absorbability α_b | 0.95 |
| Glass emissivity ϵ_g | 0.88 |
| Water emissivity ϵ_w | 0.95 |
| Basin emissivity ϵ_b | 0 |
| Glass reflectivity ρ_g | 0.0735 |
| Water ρ_w | 0 |
| Basin ρ_b | 0 |
| Thermal conductivity of basin k_b , W/m°C | 16.30 |
| Thermal conductivity of losses k_l , W/m°C | 0.039 |

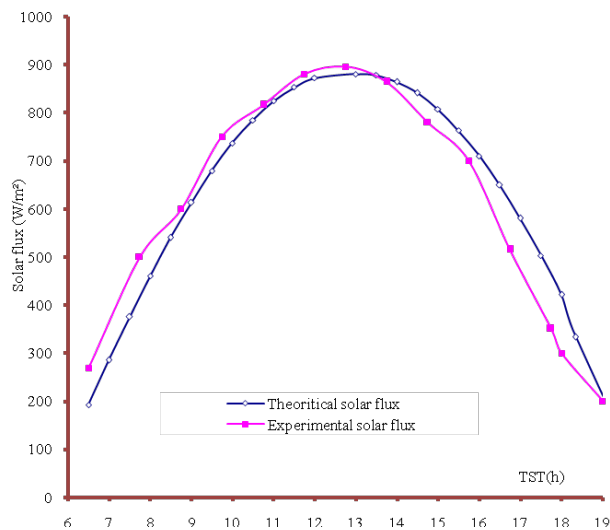


Fig. 2. Variation of experimental and calculated solar flux with respect to time (15 July 2015).

Variation of inner glass, water, and basin water and evaporator temperature recorded with respect to true solar time and represented with the help of Fig. 3. It shows that the temperature of the basin reaches 90°C in closed time intervals, that of the water temperature exceeds up to 85°C. Whereas the glass temperature remains at 20°C.

The resolution of the differential system allowed determining the temperatures at different positions of the distillers unit. Variation of the inner glass, water, basin and evaporator with respect to true solar time through the Matlab software through simulations are shown in Fig. 4.

Force circulation mode has been chosen in this study to do a comparison with the other types of solar distillation systems. This shows that the low efficiency of a conventional solar still can still be overcome by altering the operating principle as follows: Using air inside the solar still increased forced convection to the natural convection which increases the heat transfer coefficients and enhances surface water evaporation rate. Recover some of the extracted heat in the condensation process and use it to preheat the air-vapor mixture entering the water, as shown in Fig. 5, the Maximum value for the rate of convective heat transfer was evaluated 2.2W/m² °C through MATLAB simulation with an error of 4%. Which can be

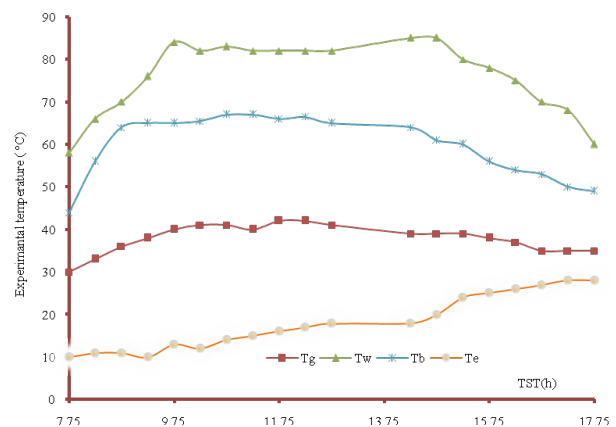


Fig. 3. Variation of experimental temperature (°C).

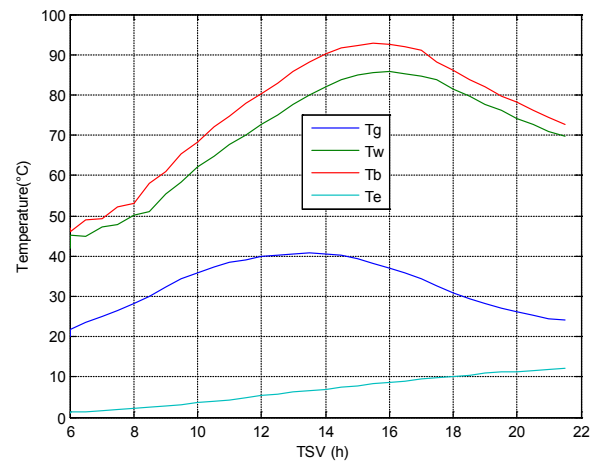


Fig. 4. Variation of theoretical temperature (°C).

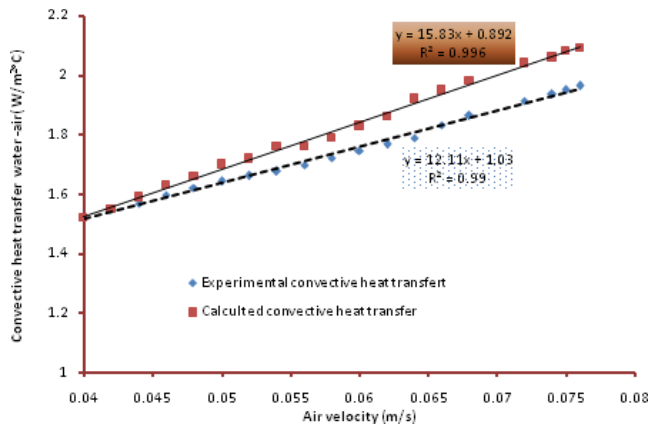


Fig. 5. Variation of convective heat transfer water-air ($W/m^2 \text{ } ^\circ C$).

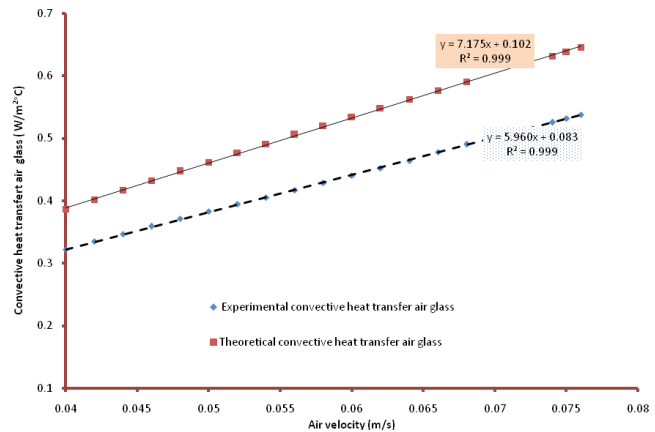


Fig. 6. Variation of convective heat transfer coefficient between air-glass ($W/m^2 \text{ } ^\circ C$).

evaluated with the relation of $y = 15.8372x + 0.8926$ and $R^2 = 0.9961$ for the experimental value $y = 12.11x + 1.09$ and $R^2 = 0.99$ can be used.

The rate of convective of heat transfer between air and glass does not exceed $0.38 W/m^2 \text{ } ^\circ C$ experimental as well as calculation with error 17%. It may be evaluated with the relation of $y = 7.1753x + 0.102$ and $R^2 = 0.9997$ for the experimental results and $y = 5.9606x + 0.0836$ and $R^2 = 0.9999$ for the theoretical results as shown in Fig. 6.

By enhancing condensation area of the flat plate covers in the standard again by the external condenser with much larger heat exchange zones to increase the condensation efficiency consequently. The results shows that the maximum rate of evaporation can be increased as the temperature due to enhancement in water temperature and maximum rise of water temperature was recorded $90^\circ C$ while the analysis. The predicted and experimental distillate output of distiller unit is shown in Fig. 7 which shows good agreement. This will give credence to developed models for performance analysis of passive and active distiller units.

The rate of production was increased due to the reduction of the inner wall of glass temperature, due to the effect of heat pump. Thus, the flow rate of the recovered distillate is more due to the temperature gradient between the water and the inner surface of the pane. The temperature difference between water and inner surface of glass cover material increases due to forced circulation of the air velocity. Which results, heat transfer rate of convective and evaporative modes increase. Indeed the simulated results have a very good agreement with the experimental results up to 14 TSV. Replace the saturated air in the ambient air with 'drier' air to increase the mass transfer potential in the image, resulting in higher outputs. Circulate the standard air vapor mixture to external water-cooled condensers to achieve efficiency from a lower condensing temperature.

6. Economic analysis

Using economic analysis, estimation of the cost of one-liter distillate water has made. In addition to the capital cost (P) of the hybrid solar still, other parameters such as sink-

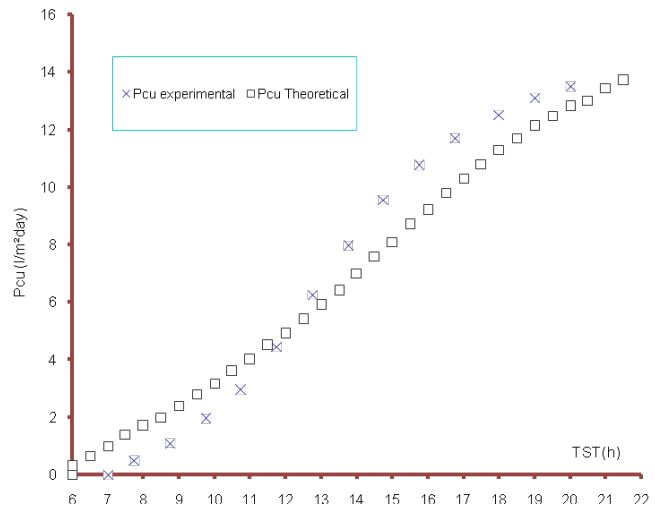


Fig. 7. Variation of experimental and theoretical cumulated productivity Pcu ($l/m^2 \text{ day}$).

ing fund factor (SFF), annual salvage value (ASV), annual maintenance cost (AMC), and interest rate per year should be also considered. At this stage, the capital recovery factor (CRF) is defined in terms of the interest per year i and also the number of life years of the system n [22,23].

$$CRF = \frac{i(1+i)^n}{(1+i)^n - 1} \tag{13}$$

The interest per year i and the number n of life years of the system are assumed 12% and 10, respectively. Fixed annual cost (FAC) becomes:

$$FAC = P(CRF) \tag{14}$$

where P is the capital cost of solar still. The capital cost includes the cost of the hybrid solar still and air compressor as well as the costs of labor cost (for the active system). In this work the capital cost P becomes 1026.

Table 3
Design parameters of hybrid solar still

| | |
|---|-------|
| Basin liner area, m ² | 0.4 |
| Basin length, m | 0.650 |
| Basin width | 0.615 |
| Glass cover emissivity | 0.9 |
| Glass cover thermal conductivity, W/m·K | 0.78 |
| Glass cover thickness, m | 0.003 |
| Glass cover inclination angle, ° | 30 |
| Glass cover area, m ² | 0.48 |
| Glass cover length, m | 0.733 |
| Glass cover width, m | 0.65 |
| Glass cover absorptivity | 0.1 |

By taking the salvage value of system S equal to 20% of capital expressed respectively as [19]:

$$SFF = \frac{i}{(1+i)^n - 1} \quad (15)$$

Sinking fund factor (SFF) and annual salvage value (ASV) can be

$$ASV = (SFF)S \quad (16)$$

$$\text{For } S = 0.2P \quad (17)$$

Sinking fund factor (SFF) and annual salvage value (ASV) can be for the passive unit, 0.0569 and 0.1769 \$ (by considering 205.20 \$ for the pump price) for the active one.

The AMC which is annual maintenance operational cost of the system consists of collecting the fresh water, cleaning the glass cover, washing inside the unit to remove the deposited salt, and maintenance of DC fan. Here, 15% of the fixed annual cost is considered as maintenance cost:

$$AMC = 0.15(FAC) \quad (18)$$

Therefore the annual cost (AC) is:

$$AC = FAC + AMC - ASV \quad (19)$$

Finally, the cost of fresh water per liter can be calculated as:

$$CPL = \frac{AC}{M} \quad (20)$$

where M is the average annual yield of the solar still.

Cost per liter of fresh water is shown in table 4 for the hybrid distiller unit with and without an air compressor.

7. Conclusion

The amplification of numerical models to determine the performance of an active solar distiller by forced convection was the objective of this work. It incorporates heat and

Table 4
Distilled water cost calculation

| Type of distiller | Annual production, kg | Annual cost (\$) | Cost per liter of fresh water/\$ |
|------------------------|-----------------------|------------------|----------------------------------|
| With air compressor | 5840 | 197.13 | 0.031 |
| Without air compressor | 3285 | 154.43 | 0.047 |

mass transfer in the forced convection mode for a solar distiller unit with heat recovery. Comparison of experimental and numerical results indicates that models can be used for prediction of distillate output for hybrid distiller unit. The values of convective heat transfer between water-air and air-glass are respectively 2.2 W/m² °C and 0.6 W/m² °C. The errors between the experimental and theoretical study it in order of 0.4% for the first case and 17% for the second case. The cumulative productivity is equal to 16 l/ m²·d

Symbols

- q_{ew} — Flux evaporation (W/m²)
- $q_{ew,w-e}$ — Flux evaporation water-evaporator (W/m²)
- $q_{ev,f}$ — Flux losses evaporator (W/m²)
- q_{cond-g} — Flux conduction glass (W/m²)
- $q_{c,b-w}$ — Flux convection basin-water (W/m²)
- $q_{c,g-a}$ — Flux convection glass-ambient (W/m²)
- $q_{c,w-g}$ — Flux convection water-glass (W/m²)
- $q_{c,w-e}$ — Flux convection water-evaporator (W/m²)
- $q_{r,g-a}$ — Flux radiation glass-ambient (W/m²)
- $q_{r,w-g}$ — Flux radiation water-glass (W/m²)
- T_w — Water temperature (°C)
- T_f — Fluid temperature (°C)
- T_g — Glass temperature (°C)
- T_b — Basin temperature (°C)
- T_e — Evaporator temperature (°C)
- TST — True solar time (h)
- Pcu — Cumulated productivity (kg/h)
- V — Air velocity (m/s)
- g — Gravity acceleration (N/kg)
- β — Inclination (°)
- μ — Dynamic viscosity (KJ/m²·K)
- Δ — Difference
- COP — Coefficient of performance

Cost nomenclature

- AC — Annual cost (\$)
- AMC — Annual maintenance operational cost of the system (\$)
- ASV — Annual salvage value
- CPL — Cost of fresh water (\$/lit)
- CRF — Capital recovery factor

References

- [1] K. Hidouri, R.B. Slama, S. Gabsi, Desalination by simple solar distiller assisted by a heat pump, J. En. Sc. Eng., 5 (2011) 1183–1188.

- [2] B.K. Biswas, M.A. Halim, S. Parvin, B.H. Mandal, M.W. Rahman, M.J. Alam, K.M.S. Islam, Experimental study of the operational parameters on low-cost single-basin solar still in Jessore, Bangladesh, *J. Chem. Eng.*, 29 (2017) 3–8.
- [3] G.N. Tiwari, S.P. Gupta, A. Kumar, Analytical model of inverted multiwick solar still, *Int. J. Solar Energy*, 6 (1987) 139–150.
- [4] G.C. Pandey, Effect of dried and forced air bubbling on the partial pressure of water vapour and performance of solar still, *Solar Eng.*, 33 (1984) 13–18.
- [5] K. Srithar, T. Rajaseenivasan, Performance analysis on a solar bubble column humidification dehumidification desalination system, *Process Safety Environ. Protect.*, 105 (2017) 41–50.
- [6] T. Koyuncu, Performance of various designs of solar air heaters for crop drying applications, *Ren. Eng.*, 31 (2006) 1073–1088.
- [7] K.K. Matrawy, Theoretical analysis for an air heater with a box-type absorber, *Sol. Eng.*, 63 (1998) 191–198.
- [8] N.T. Bao, Numerical modelling of basin type solar still mechanics, *Mater. Sci. Eng.*, 4 (2016) 133–147.
- [9] M. Zerrouki, N. Settou, Y. Marif, M.M. Belhadj, Simulation study of a capillary film solar still coupled with a conventional solar still in south Algeria, *Energy Convers. Manage.*, 85 (2014) 112–119.
- [10] K. Rajasekar, R. Pugazhenth, A. Selvaraju, T. Manikandan, R. Saravanan, Effect on air quality and flow rate of fresh water production in humidification and dehumidification system, *Mater. Sci. Eng.*, 183 (2017) 12–32.
- [11] A.E. Kabeel, M.M. Bassuoni, M. Abdelgaied, Experimental study of a novel integrated system of indirect evaporative cooler with internal baffles and evaporative condenser, *Energy Convers. Manage.*, 138 (2017) 518–525.
- [12] G. Mink, M.M. Aboabboud, E. Karmazsin, Air blown solar still with heat recycling, *Solar En.*, 4 (1998) 309–317.
- [13] A.E. Kabeel, M. Abdelgaied, M. Mahgoub, The performance of a modified solar still using hot air injection and PCM, *Desalination*, 379 (2016) 102–107.
- [14] K. Hidouri, S. Gabsi, Correlation for Lewis number for evaluation of mass flow rate for simple/hybrid solar still, *Desal. Water Treat.*, 57(14) (2016) 6209–6216.
- [15] N. Hidouri, K. Hidouri, R.B. Slama, S. Gabsi, Effects of the simple/double glass cover use and the orientation of a simple solar still on operating parameters, *Desal. Water Treat.*, 36 (2011) 383–391.
- [16] M.S. Sodha, D.R. Mishra, A.K. Tiwari, Solar earth water still for highly wet ground, *J. Fundam. Ren. En Appl.*, 4 (2014) 1–2.
- [17] K. Hidouri, D.R. Mishra, A. Benhmidene, B. Chouachi, Experimental and theoretical evaluation of a hybrid solar still integrated with an air compressor using ANN, *Desal. Water Treat.*, 88 (2017) 52–59.
- [18] S.K. Shukla, S.K. Singh, S.K. Gupta, Analytical study and optimization of thermal performance of flat plate solar air heater, *J. Sust. Manuf. Renew. En.*, 1 (2012) 49–63.
- [19] D.R. Mishra, A.K. Tiwari, M.S. Sodha, Mathematical modeling and evaluation of new long single slope still for utilization of hot waste water., *Appl. Therm. Eng.*, 108 (2016) 353–357.
- [20] H. Panchal, I. Mohan, Various methods applied to solar still for enhancement of distillate output, *Desalination*, 415 (2017) 76–89.
- [21] J.A. Duffie, W.A. Beckman, *Solar Engineering of Thermal Processes*. Laboratory University of Wisconsin-Madison Copyright 2013 by John Wiley & Sons, Inc.
- [22] J.A. Esfahani, N. Rahbar, M. Lavvaf, Utilization of thermoelectric cooling in a portable active solar still - An experimental study on winter days, *Desalination*, 269 (2011) 189–205.
- [23] A.E. Kabeel, A.M. Hamed, S.A. El-Agouz, Cost analysis of different solar still configurations, *Energy*, 35 (2010) 2901–2908.

Annexes

$$h_{r,x-y} = \frac{\epsilon_g \sigma [(T_x)^4 - (T_y)^4]}{(T_x - T_y)}$$

where x and y are variables associated with the desired temperature working

$$q_{r,g-a} = h_{r,g-s} (T_g - T_s)$$

$$q_{r,w-g} = h_{r,w-g} (T_w - T_g)$$

$$q_{c,g-a} = h_{c,g-a} (T_g - T_a) = 5.7 + 3.8 \sqrt{V(T_g - T_a)}$$

$$q_{losses(b)} = U_b (T_b - T_a) = \frac{\lambda_b}{e_b} (T_b - T_a)$$

$$h_{c,x-y} = 0.884 \left[(T_x - T_y) + \left(\frac{(P_x - P_y)(273 + T_x)}{268.9 \cdot 10^3 - P_x} \right) \right]^{1/3}$$

where x and y variables

$$q_{c,w-g} = h_{c,w-g} (T_w - T_g)$$

$$q_{c,w-e} = h_{c,w-e} (T_w - T_e)$$

$$q_{ev,w-f} = h_{ev,w-f} (T_w - T_e)$$

$$\begin{cases} h_{c,b-w} = 0.54 \frac{k_w \cdot Ra^{1/4}}{L} \text{ if } 10^4 \leq Ra \leq 10^7 \\ h_{c,b-w} = 0.15 \frac{k_w Ra^{1/3}}{L} \text{ if } 10^7 \leq Ra \leq 10^{11} \end{cases}$$

$$q_{ev,f} = h_{ev,f} (T_e - T_f) / h_{ev,f} = \frac{Nu \cdot k}{L}$$

$$q_c = \frac{COP \cdot W}{S}$$

$$Gr = \frac{\beta_{ex} g \rho_f^2 L^3 \Delta T}{\mu_f^2} Pr = \frac{\mu_f C_{Pa}}{\lambda_f}$$